Hindawi
Advances in Materials Science and Engineering
Volume 2019, Article ID 8680715, 8 pages
https://doi.org/10.1155/2019/8680715

Review Article

FIB-SEM Three-Dimensional Tomography for Characterization of Carbon-Based Materials

Nan Nan and Jingxin Wang

Division of Forestry and Natural Resources, Davis College of Agriculture, Natural Resources and Design, West Virginia University, Morgantown, WV 26505, USA

Correspondence should be addressed to Jingxin Wang; jxwang@wvu.edu

Received 12 April 2019; Revised 14 June 2019; Accepted 27 June 2019; Published 21 July 2019

Guest Editor: Anita Andicsová Eckstein

A review on the recent advances of the three-dimensional (3D) characterization of carbon-based materials was conducted by focused ion beam-scanning electron microscope (FIB-SEM) tomography. Current studies and further potential applications of the FIB-SEM 3D tomography technique for carbon-based materials were discussed. The goal of this paper is to highlight the advances of FIB-SEM 3D reconstruction to reveal the high and accurate resolution of internal structures of carbon-based materials and provide suggestions for the adoption and improvement of the FIB-SEM tomography system for a broad carbon-based research to achieve the best examination performances and enhance the development of innovative carbon-based materials.

1. Introduction

In the past couple of decades, various carbon-based materials and their applications have been rapidly developed and they have played an important role in modern material sciences. Especially, the utilizations of inexpensive and sustainable carbon materials have been extensively studied for renewable energy storage (e.g., supercapacitors [1–5] and batteries [6–8]), adsorbent (e.g., soil amendment [9–11], water purification [12–14], and gas separation [15–18]), composites with enhanced certain properties (e.g., thermal and mechanical enhancement) [19–22], and catalysts of fuel cells [23] and other chemical reactions [24, 25]. Therefore, along with the electrochemical, chemical, and mechanical properties, it is vital to investigate and further optimize or control the morphologies and internal structural features of the versatile carbon-based materials through design, synthesis, and improvement steps.

To support the advanced product design and processing, three-dimensional (3D) and geometry-sensitive features of the carbon-based materials are desired. However, the most commonly used scanning electron microscope (SEM) technique is only able to reveal the features on surface of the materials. Transmission electron microscopy (TEM) may be an option and great for characterization at nanoscale, but it is difficult to process the appropriate samples and could be expensive to perform. X-ray tomography allows three-dimensional quantitative measurements with the advantages of nondestruction and relatively high spatial resolution, but due to the restriction on the penetration ability of X-ray, it is not a good option for high-density and large-volume samples [26].

The focused ion beam-scanning electron microscope (FIB-SEM) system is a new approach to investigate the three-dimensional internal structures of various materials because of its good performance and easy process. There are almost no limitations on the specimen materials using this technique [27]. A completed FIB-SEM 3D tomography analysis includes three main sections: FIB-SEM processing, imaging analysis, and quantitative 3D reconstruction. FIB is used for serial sectioning/milling the sample, and SEM can image the exposed cross-sectional region (Figure 1). The FIB and SEM beams have coincident angles of 52/54° (in the current commercial type). Milling rates (ion-beam acceleration voltage and current) in FIB can be varied depending

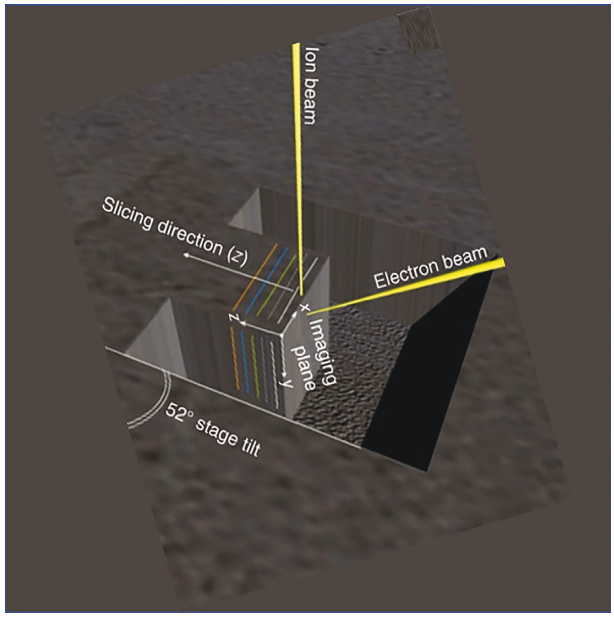

Figure 1: The schematic diagram of the FIB-SEM system [26].

on the difference in hardness and geometrical rigid integrity of the sample materials. After the FIB-SEM process, the software (e.g., Avizo) continues to analyze generated data and conduct 3D reconstruction to obtain quantitative 3D tomography results (Figure 2). Additionally, FIB instruments can be equipped with electron dispersive spectroscopy (EDS) and electron back-scatter diffraction (EBSD) collection systems, allowing for chemical, crystallographic, and topological data to be obtained on each slice [28, 29].

The FIB-SEM 3D tomography technology is expected to help advance the research in carbon-based materials. This paper provides an overview of the current status of the FIB-SEM system in carbon-based material science research, discusses the further potential applications of FIB-SEM in carbon and carbon-based materials, including methodology, crucial parameters, and problems and corresponding solutions, and concludes with an assessment of the promising role of the FIB-SEM 3D tomography technique in development of advanced innovative carbon-based materials.

2. FIB-SEM 3D Tomography in Current Carbon-Based Material Studies

In recent years, the FIB-SEM tomography system has been tentatively applied to characterize the microstructures of some carbon-based materials used for the applications of batteries, supercapacitors, and fuel cells. Table 1 lists the majority of carbon-based material studies that used the FIB-SEM tomography system. Generally, in the previous carbon-based material studies, the utilizations of FIB-SEM systems can be classified into two major categories including the 2D observation of the FIB-SEM cross-section images and the visual and quantitative analyses using the 3D reconstruction of the stacking of FIB-SEM cross-section images.

2.1. 2D Observation of FIB-SEM Cross-Sectional Images. FIB-SEM tomography is a very useful approach to investigate the subsurface imaging of various materials. Compared to the conventional SEM that only focuses on the surface morphology, FIB-SEM is able to provide more information of the internal structures through analyzing the 2D cross-sectional images. FIB-SEM is ideally suited for the characterization of micron and submicron scale to a minimum resolution values of about 10–15 nm [26]. The limitations of this technique make it difficult to image the structure that is smaller than 5–10 nm [43]. Figure 3 shows the resolution ranges for several modern tomography methods to meet the needs of different research purposes.

The FIB-SEM has been used to investigate the subsurface images in current studies of carbon-based materials. For instance, Rodriguez et al. [41] used the FIB-SEM to observe the open three-dimensional structure of the modified hierarchical nanoporous carbon (Figure 4(a)). In the study of Yürüm et al. [40], FIB-SEM showed a clear layer of iron oxide particles covering oxidized activated carbon and they found that the uniform layers can rapidly be grown through the microwave hydrothermal synthesis. Zhang et al. [48] showed the core-shell and yolk-sell nanostructures of carbon spheres using FIB-SEM. Ogihara et al. [36] found that the cross-sectional FIB-SEM images of the electrodes indicated that 2,6-Naph$(COOLi)_2$ particles were covered with conductive nanocarbon and revealed uniform pore structures in the internal. When Liu et al. [31] hybridized graphene in Ni foam using chemical vapor deposition, the FIB-SEM images showed the graphene grown on Ni foam, and the Wrinkle-like graphene with irregular fractures was found to fully cover the Ni foam skeleton. Singh et al. [32] observed the clearly visible interconnected porous layer of nanoporous gold in the pristine nanoporous gold layer with a thickness of ca. 130 nm. The thickness of nanoporous gold-nitrogen-doped carbon nano-onion layer was ca. 750 nm. Shen et al. [33] used FIB-SEM tomography analyses to confirm the fine structure of graphite fluoride-lithium fluoride-lithium (GF-LiF-Li) composite and observed that the GF-LiF-Li composite was composed of three layers, including the top GF-LiF layer, followed by a transitional zone consisting of GF, LiF, and Li metals and a bottom layer consisting solely of Li metal.

2.2. 3D Reconstruction of FIB-SEM Sequential Cross-Sectional Images. Due to limited information extracted from two-dimensional features, the 2D observation cannot be compared to three dimensional and geometry-sensitive features. To reveal the real physical characterization of an element/material and support advanced study, design, and process development, a higher dimensional technology with holistic and accurate information is needed. The FIB-SEM 3D tomography enables the direct observation of the three-dimensional microstructure at nanoscale resolution through the 3D reconstruction of the sequential sets of 2D images. Furthermore, owing to recent advances in imaging and computer technology, numerical simulation based on FIB-SEM 3D tomography technique is one of the most accurate

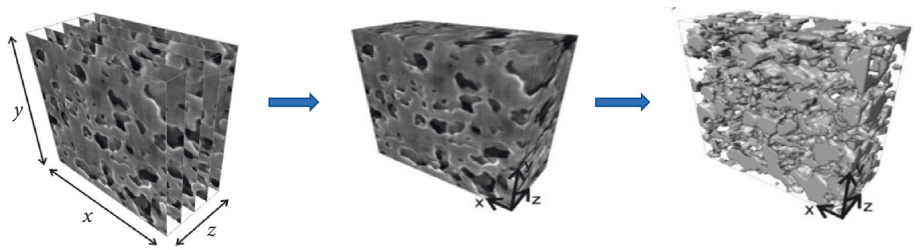

(a) (b) (c)

Figure 2: The procedures of FIB-SEM 3D reconstruction. (a) Stack of images produced with FIB-SEM, (b) imaging 3D reconstruction, and (c) quantitative 3D reconstruction and modeling [30].

Table 1: Short indicative selection of FIB-SEM for carbon-based materials from the literature.

Material	Application	Methodology	Purpose	Year	Reference
Hybrid graphene on Ni foam	Electrode of supercapacitors	Dual Beam Strata 235 (FEI) and Auriga Compact (Zeiss) microscope	To analyze the morphologies and structural features of the composites	2019	[31]
Nanoporous gold-nitrogen-doped carbon nano-onions	Electrode of micro-supercapacitor	FIB-FEG-SEM of Carl Zeiss Auriga Compact-4558	To determine the thickness of the different layers present in the electrode	2019	[32]
Graphite fluoride-lithium	Lithium battery	FIB-SEM, Scios, FEI	To confirm the fine structure of GF-LiF-Li composite	2019	[33]
Carbon nanofiber	Supercapacitor	Auriga Cross Beam, Zeiss Software: Avizo 9.0.0	To examine fiber subsurface microstructure	2018	[34]
Coal	Fuel	FEI Helios Nanolab 650 FIB-SEM system	To quantitative evaluate the 3D characterization of pore-fracture networks of coals	2017	[35]
Conductive carbon black/carbon fiber coating	2,6-Naph$(COOLi)_2$ electrodes	FIB: 50 nA current and 7 kV acceleration voltage SEM: operating at 2 kW.	To investigate the nanocarbon coating and the uniformness of pore structures	2016	[36]
Nanoporous carbon-binder	Li-ion batteries	Zeiss Auriga 60 dual beam: 20 pA current, 30 kV acceleration voltage, and 9 nm cutting distance	To reconstruct the carbon-binder domain of a $LiCoO_2$ battery cathode	2015	[37]
Carbon nanotubes (CNTs) in polymer composites	Nanotechnology	SEM: 5 kV, pixel size of 3 nm FEI Helios Nanolab 600 FIB-SEM system	To investigate the subsurface imaging of CNTs	2015	[38]
Porous carbon-based electrode	Electrode	FIB: 80 pA current and 30 kV acceleration voltage SEM: 3 kV voltage The voxel size was $10 \times 10 \times 10\ nm^3$ Software: IMOD, ImageJ, and AVIZO software	To analyze the morphologies and build topographic reconstruction of the porous carbon electrode	2014	[39]
Deposition of porous iron oxide on activated carbon (AC)	Adsorbent	FIB: 10–1 nA current and 30 kV acceleration voltage SEM: 2–5 kV voltage	To understand the nature of iron oxide particles within the pores of AC	2014	[40]
Hierarchical nanoporous carbon synthesized using a hard template method	Electrode	Dual-beam workstation FEI Helios Nanolab 600; a field emission gun SEM	To observe the open 3D porous structure of the carbon	2013	[41]
Nanoporous carbon-supported noble metal catalyst layers	Fuel cells	FIB: 50 pA current and 30 kV acceleration voltage SEM: 2 kV voltage	To characterize porosity, connectivity, and pore-size and grain-size distribution	2013	[42]
Disordered mesoporous carbon with tailored pore size	Fuel cells supercapacitors	FIB: 27 pA current and 30 kV acceleration voltage SEM: 86 pA current and 5 kV voltage The voxel size was $3.57 \times 3.62 \times 10\ nm^3$ Software: Amira® 5.2 software and MAVI	To visualize and study nonordered pore morphology and quantitatively characterize their physical properties	2013	[30]

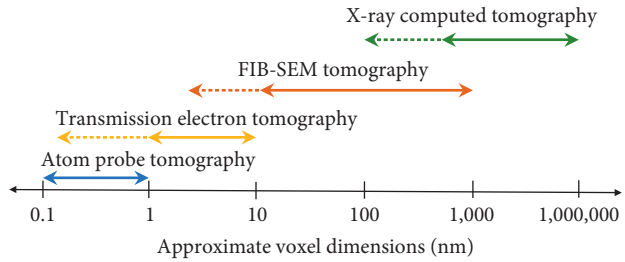

FIGURE 3: The resolution of modern tomographic characterization methods is displayed as an approximate range. Dash lines represent advanced potential range [26, 43–47].

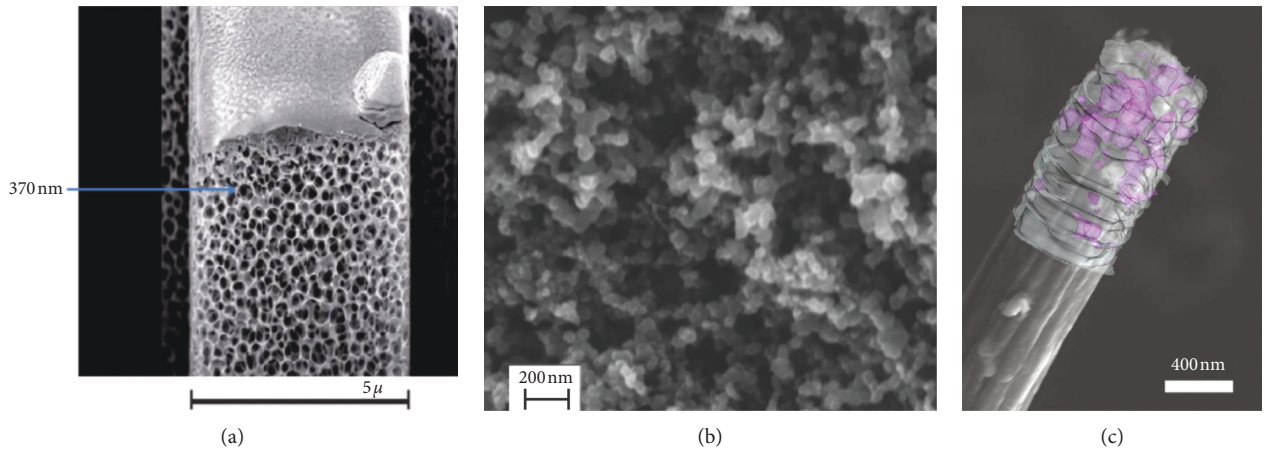

FIGURE 4: FIB-SEM images. (a) Cross-sectional SEM image of a SiO_2 nanoparticle [41], (b) SEM image of microstructure of porous carbon electrode [39], and (c) reconstructed FIB-SEM image applied onto the SEM of a single nanofiber [34].

and effective tools to investigate the nature of material internal structures, such as porous structures [27, 49, 50], phase distribution, crystallographic interfaces, and defect arrangements [26]. However, the quantification errors in the microstructural parameters are inevitable because of the limited sample size and resolutions in the FIB-SEM observation, uncertainty in the image processing (e.g., alignment and segmentation), and the accuracy of the quantification method/model itself applied to the image data [51]. Rapidly advanced FIB, high-resolution SEM, and other observation techniques will assist to mitigate these errors.

Although it is rare, 3D reconstruction using FIB-SEM has been used in several studies of carbon-based materials. For instance, Balach et al. [30] performed a direct and quantitative 3D reconstruction of the internal structure of disordered mesoporous carbon using serial sectioning FIB-SEM with an ion beam current of 27 pA at 30 kV. The samples were reconstructed by the Amira® 5.2 software from 25 slices (~10 nm thickness per slice) obtained and further quantitatively analyzed by the software system's Modular Algorithms for Volume Images (MAVI). The total analyzed volume (VT) of material was 0.0625 μm^3. Their results indicated that FIB-SEM was only able to reveal the 3D shape, distribution, and connectivity of mesopores, since the resolution of SEM was not sufficient for access to pores with a diameter below 2 nm. The structural parameters of the pores including surface area, pore volume, Euler number, total porosity, and pore size distribution were determined through the 3D reconstruction analysis. Eswara-Moorthy et al. [39] performed a 3D reconstruction of the porous carbon-based electrode using FIB-SEM with an ion beam current of 80 pA at 30 kV (Figure 4(b)). They found that the Pt filling of the pores drastically improved the image contrast between the carbon and the porous phases, and the enhanced image contrast enabled robust semiautomatic demarcation of the interfacial boundaries and subsequent binarization of the images with very high fidelity. Also, through analyzing the 3D reconstruction, the porosity ($72 \pm 2\%$), axial and radial tortuosites (1.45 ± 0.04 and 1.43 ± 0.04), average pore size (90 nm), pore-size-distribution (20–300 nm), surface-to-volume ratio (46.5 μm^{-1}), and specific surface area (13.0 μm^{-1}) were determined. Their results indicated that porous carbon-based electrode has a very high surface area, which can be more conducive for surface electrochemical reactions. Thiele et al. [42] reported that the FIB-SEM only differentiated the pores and total solid phase from each other, but it was not possible to further differentiate the solid phase into carbon, ionomer, and Pt nanocomponents. FIB-SEM analysis revealed a preferential size in the grain-size-distribution (GSD) of about 65 nm and the pore-size-distribution (PSD) showed highly porous material characteristics with 58% porosity and pores ranging from 7 nm to 350 nm, and 99.9% of the pore area was connected. Liu et al. [34] reconstructed the carbon nanofiber

using FIB-SEM, and the internal MnO particles showed some degree of agglomeration within the fiber (Figure 4(c)). Additionally, the FIB-SEM system was used to characterize microstructural features for three dimensions of carbides in Ni-based high carbon alloy [52] and nanoporous carbon-binder of Li-ion batteries [37].

3. Potential Applications of FIB-SEM 3D Tomography in Carbon-Based Material Studies

To meet the different requirements of various applications for characterization of carbon-based materials, the FIB-SEM 3D tomography will be likely be used to reveal the features or phenomenon in a variety of application fields. It is very valuable to know the potential use of FIB-SEM, what it can do, and possible problems and practical solutions for each specific application.

3.1. Carbons. Tomographic methods using serial-sectioning and imaging processes are suitable for observing the morphology and internal microstructure of carbons, such as graphene, carbon nanotube, carbon black, activated carbon, and biochar, which are extensively used in various applications, for example, quantitative evaluation of the 3D characterization of pore-fracture networks of coals [35], mesoporous carbon [30], and carbon fiber [34]. Moreover, various parameters that are relevant to the microstructures can be numerically evaluated by using the FIB-SEM tomography and implementing 3D reconstruction of serial stacking sectioned SEM images, including surface texture (e.g., roughness), different particle sizes and distribution, and connectivity (pore tortuosity) of the internal material.

In the FIB process, carbons can be classified by volume size. If the initial size of carbon (e.g., a monolithic carbon) is bigger than the best operation range for FIB-SEM, the sample will be adjusted to a proper size for testing. While if the initial size is too small to test by a single sample (e.g., micro/nanocarbon fibers, particles, and nanotubes), a potential method is to cast one or more carbons into a support matrix, such as, epoxy resin [27]. This methodology has been demonstrated by studies of various hierarchical porous materials, such as, zeolite beads [27], silicon [53], monolithic UiO-66-NH2 material [54], and concrete [46].

The curtain effect may occur in the milling process, which appears as parallel scratches varying in the same direction of ion beam milling and making the image appears to be covered by a semitransparent curtain [27, 55, 56]. The potential reasons are as follows: (1) roughness of the slicing surface varies the angles of the ion beam and causes the differences of the milling rate, and depositing protection layers may mitigate the surface roughness; (2) different characteristics of the elements in the targeting materials can cause curtain effect as well; (3) presence of internal pores in the samples can change the intensity or pathway of ion beam when it passes through the pores. Therefore, currently, the most common and effective curtain-removal solution is adjusting the milling parameters according to the unique properties of each targeted material or polishing it before milling. Filling the internal pores with additional resin can help recognize the pore region [49, 50].

3.2. Carbon-Based Electrodes. Due to the high energy-to-weight ratio, surface area, conductivity, and micro/nanoporous structure of carbons, porous carbon-based electrodes for the use of various supercapacitors and batteries have gained more attentions recently. Furthermore, porous carbon-based composite electrodes can display both capacitive and faradaic charge storages. Also, carbon electrodes can be involved in much more complex designs to improve the energy density of supercapacitors/batteries [4]. Therefore, it is crucial to accurately examine the porous structures of carbon-based electrodes.

The 3D microstructure of porous electrodes can be investigated by FIB-SEM tomography. The respective morphological characteristics/parameters, volume fraction, spatial distribution, size, connectivity, and tortuosity, can be determined through analyzing the obtained 3D reconstruction using image processing software and modeling. For example, the common used software for image processing includes IMOD, ImageJ [39], Fiji [57], Avizo [34, 35], and Amira 5.5.0 [30, 57]. The algorithm tools for quantification analysis are lab-made MATLAB [58] and Java [59]. The existing reported studies that used the FIB-SEM quantitative 3D reconstruction are porous carbon-based electrode [54], carbon nanofiber based supercapacitor [49], and mesoporous carbon electrode material [56].

3.3. Carbon-Based Catalyst/Coating/Hybrid Layers. The FIB-SEM 3D tomography technique is a useful method for the diagnosis of the catalyst [56, 60], coating [61], or hybrid [31] layer structure as well. It can reconstruct the geometrical properties of the catalyst layer in 3D space. The digital analysis can assist to determine the porosity and the permeability. Also, it is a simple and effective way to understand the degradation mode of the catalyst layer.

The heating/fusion damage may occur in the milling process. It can thermally damage the catalyst layer(s). The liquid nitrogen cooling and thermoelectric cooling via Peltier elements methods have been demonstrated and proved that they can mitigate the heating damage [56]. The thermoelectric cooling is considered to exceed the liquid nitrogen cooling since the thermoelectric cooling enables a short-time sample fabrication at the FIB stage.

3.4. Carbon-Based Polymer Composites. Carbon-based polymer is the most common type of the polymer composites. The addition of carbon fillers likely enhances the certain properties of the polymer to some degrees; for instance, the biochar particle-filled PVA films obtained improved thermal stability, electrical conductivity, and mechanical properties, but the tensile strength of the films was reduced dramatically as the increase of biochar content due to the particle aggregation and porous features of the biochar [20, 62]. Therefore, it is important to investigate the structural

features of the carbon filler and polymer matrix to obtain good designs for fabricating the composites.

The 3D reconstruction using FIB-SEM can be applied to study the dispersion of the carbon filler inside a polymer matrix and the morphology and internal structure of the carbon filler and/or to determine the effect of interphase properties on mechanical properties of nanocomposites [63]. However, several problems can occur during the milling process.

These problems can occur in all types of materials but are more detrimental in polymer composites due to the characteristics of the polymer matrix, such as low thermal conductivity, thermal melt and decomposition temperatures, and mechanical properties. First, the heating damage is always a concern. Cracking caused by the heat produced during processing cannot be dissipated through the low thermal conductive polymer and generates stress to break the polymer with lower mechanical properties. The second one is material redisposition caused by the melt of polymer. The third problem is the curtain effect. The excessive heat can damage the surroundings and leave holes on the sectional surface. Nonetheless, it is possible to mitigate these problems in several ways. As mentioned above, the proper cooling approaches can be applied to prevent the overheating. Also, another option is to directly reduce the energy of heating source, such as ion beam current deduction and acceleration voltage deduction.

4. Summary and Outlook

The FIB-SEM 3D tomography has been applied in the investigation of morphologies and internal structural features of carbon-based materials, especially carbon-based electrodes. However, the utilizations of FIB-SEM 3D tomography in carbon-based materials are still limited, particularly in quantitative 3D reconstruction-related studies. We noticed that it is possible to extend the FIB-SEM 3D tomography to more applications of carbon-based materials, and highly potential areas are the studies in carbons, carbon-based various electrodes, catalyst, coating, or hybrid layers, and polymer composites. However, the digital analyses and modeling mainly relied on the design and coding by researchers, which are difficult to be used as broad as the commercialized software due to the complexity and low versatility of the existing methods. A simple, integrated, and powerful analysis system for both visible and quantitative 3D reconstruction and analysis will further promote the utilization of FIB-SEM tomography. Moreover, to mitigate the quantification errors in the microstructural parameters caused by the limited sample size and resolutions in the FIB-SEM observation, uncertainty in the image processing, and the accuracy of the quantification method itself, the advanced FIB, high-resolution SEM, and powerful data-processing techniques are desired in further studies.

Furthermore, currently, FIB-SEM 3D tomography was only used to reveal the microstructure of the materials, which blocks the development of FIB-SEM as well. For plenty of carbon-based materials, the nanostructures are more important, and TEM can perform better at nanoscale. One solution is to combine the FIB-SEM and TEM to obtain the 3D micro- and nanostructures, which has been successfully performed in some studies. Another way is to improve the resolution of SEM. A super asymmetric resolution of 3D imaging technique has been reported for nano- and mesoscale morphologies [64].

The FIB-SEM tomography is becoming a routine technique to obtain 3D information on a variety of materials. With the rapid development of FIB-SEM 3D tomography, the enhanced 3D reconstruction technique is most likely to play a significant role in future characterization of carbon-based materials to further improve the products and optimize their performance, reliability, productivity, and production costs.

Conflicts of Interest

The authors declare that they have no conflicts of interest.

Acknowledgments

This work was supported by the Renewable Materials and Bioenergy Research Center in the Division of Forestry and Natural Resources at West Virginia University.

References

[1] Q. Ke and J. Wang, "Graphene-based materials for supercapacitor electrodes—a review," *Journal of Materiomics*, vol. 2, no. 1, pp. 37–54, 2016.

[2] Q. Wang, J. Yan, and Z. Fan, "Carbon materials for high volumetric performance supercapacitors: design, progress, challenges and opportunities," *Energy & Environmental Science*, vol. 9, no. 3, pp. 729–762, 2016.

[3] P. A. Basnayaka and M. K. Ram, "A review of supercapacitor energy storage using nanohybrid conducting polymers and carbon electrode materials," in *Conducting Polymer Hybrids*, V. Kumar, S. Kalia, and H. C. Swart, Eds., pp. 165–192, Springer International Publishing, Cham, Switzerland, 2017.

[4] A. Borenstein, O. Hanna, R. Attias, S. Luski, T. Brousse, and D. Aurbach, "Carbon-based composite materials for supercapacitor electrodes: a review," *Journal of Materials Chemistry A*, vol. 5, no. 25, pp. 12653–12672, 2017.

[5] Z. Gao, Y. Zhang, N. Song, and X. Li, "Biomass-derived renewable carbon materials for electrochemical energy storage," *Materials Research Letters*, vol. 5, no. 2, pp. 69–88, 2017.

[6] M.-S. Balogun, Y. Luo, W. Qiu, P. Liu, and Y. Tong, "A review of carbon materials and their composites with alloy metals for sodium ion battery anodes," *Carbon*, vol. 98, pp. 162–178, 2016.

[7] M. Keppeler, N. Shen, S. Nageswaran, and M. Srinivasan, "Synthesis of α-Fe_2O_3/carbon nanocomposites as high capacity electrodes for next generation lithium ion batteries: a review," *Journal of Materials Chemistry A*, vol. 4, no. 47, pp. 18223–18239, 2016.

[8] J. Liang, Z.-H. Sun, F. Li, and H.-M. Cheng, "Carbon materials for Li–S batteries: functional evolution and performance improvement," *Energy Storage Materials*, vol. 2, pp. 76–106, 2016.

[9] S. Steinbeiss, G. Gleixner, and M. Antonietti, "Effect of biochar amendment on soil carbon balance and soil microbial

activity," *Soil Biology and Biochemistry*, vol. 41, no. 6, pp. 1301–1310, 2009.

[10] J. H. Windeatt, A. B. Ross, P. T. Williams, P. M. Forster, M. A. Nahil, and S. Singh, "Characteristics of biochars from crop residues: potential for carbon sequestration and soil amendment," *Journal of Environmental Management*, vol. 146, pp. 189–197, 2014.

[11] T. Xie, B. Y. Sadasivam, K. R. Reddy, C. Wang, and K. Spokas, "Review of the effects of biochar amendment on soil properties and carbon sequestration," *Journal of Hazardous, Toxic, and Radioactive Waste*, vol. 20, no. 1, article 04015013, 2016.

[12] S. Wong, N. Ngadi, I. M. Inuwa, and O. Hassan, "Recent advances in applications of activated carbon from biowaste for wastewater treatment: a short review," *Journal of Cleaner Production*, vol. 175, pp. 361–375, 2018.

[13] M. I. Inyang, B. Gao, Y. Yao et al., "A review of biochar as a low-cost adsorbent for aqueous heavy metal removal," *Critical Reviews in Environmental Science and Technology*, vol. 46, no. 4, pp. 406–433, 2016.

[14] Ihsanullah, A. Abbas, A. M. Al-Amer et al., "Heavy metal removal from aqueous solution by advanced carbon nanotubes: critical review of adsorption applications," *Separation and Purification Technology*, vol. 157, pp. 141–161, 2016.

[15] A. F. Ismail and L. I. B. David, "A review on the latest development of carbon membranes for gas separation," *Journal of Membrane Science*, vol. 193, no. 1, pp. 1–18, 2001.

[16] W. N. W. Salleh, A. F. Ismail, T. Matsuura, and M. S. Abdullah, "Precursor selection and process conditions in the preparation of carbon membrane for gas separation: a review," *Separation & Purification Reviews*, vol. 40, no. 4, pp. 261–311, 2011.

[17] M. Soleimani, G. Gholami, and M. T. Ravanchi, "Application of carbon membranes for gas separation: a review," *Journal of Industrial Research & Technology*, vol. 3, no. 1, pp. 53–58, 2013.

[18] M. N. Nejad, M. Asghari, and M. Afsari, "Investigation of carbon nanotubes in mixed matrix membranes for gas separation: a review," *ChemBioEng Reviews*, vol. 3, no. 6, pp. 276–298, 2016.

[19] F. Li, Y. Liu, C.-B. Qu et al., "Enhanced mechanical properties of short carbon fiber reinforced polyethersulfone composites by graphene oxide coating," *Polymer*, vol. 59, pp. 155–165, 2015.

[20] N. Nan, D. B. DeVallance, X. Xie, and J. Wang, "The effect of bio-carbon addition on the electrical, mechanical, and thermal properties of polyvinyl alcohol/biochar composites," *Journal of Composite Materials*, vol. 50, no. 9, pp. 1161–1168, 2016.

[21] Y.-H. Zhao, Y.-F. Zhang, S.-L. Bai, and X.-W. Yuan, "Carbon fibre/graphene foam/polymer composites with enhanced mechanical and thermal properties," *Composites Part B: Engineering*, vol. 94, pp. 102–108, 2016.

[22] A. Karaipekli, A. Biçer, A. Sarı, and V. V. Tyagi, "Thermal characteristics of expanded perlite/paraffin composite phase change material with enhanced thermal conductivity using carbon nanotubes," *Energy Conversion and Management*, vol. 134, pp. 373–381, 2017.

[23] B. Fang, B. A. Pinaud, and D. P. Wilkinson, "Carbon-supported Pt hollow nanospheres as a highly efficient electrocatalyst for the oxygen reduction reaction," *Electrocatalysis*, vol. 7, no. 4, pp. 336–344, 2016.

[24] G. Wu, A. Santandreu, W. Kellogg et al., "Carbon nanocomposite catalysts for oxygen reduction and evolution reactions: from nitrogen doping to transition-metal addition," *Nano Energy*, vol. 29, pp. 83–110, 2016.

[25] J. Zhang, L. Qu, G. Shi, J. Liu, J. Chen, and L. Dai, "N,P-codoped carbon networks as efficient metal-free bifunctional catalysts for oxygen reduction and hydrogen evolution reactions," *Angewandte Chemie International Edition*, vol. 55, no. 6, pp. 2230–2234, 2016.

[26] S. N. Monteiro and S. Paciornik, "From historical backgrounds to recent advances in 3D characterization of materials: an overview," *Journal of Minerals, Metals & Materials Society*, vol. 69, no. 1, pp. 84–92, 2017.

[27] K. Bae, J. W. Kim, J.-W. Son et al., "3D evaluation of porous zeolite absorbents using FIB-SEM tomography," *International Journal of Precision Engineering and Manufacturing-Green Technology*, vol. 5, no. 2, pp. 195–199, 2018.

[28] B. Munch, P. Gasser, L. Holzer, and R. Flatt, "FIB-nanotomography of particulate systems—part II: particle recognition and effect of boundary truncation," *Journal of the American Ceramic Society*, vol. 89, no. 8, pp. 2586–2595, 2006.

[29] M. A. Groeber, *Development of an Automated Characterization-Representation Framework for the Modeling of Polycrystalline Materials in 3D*, Ohio State University, Columbus, OH, USA, 2007.

[30] J. Balach, F. Soldera, D. F. Acevedo, F. Mücklich, and C. A. Barbero, "A direct and quantitative three-dimensional reconstruction of the internal structure of disordered mesoporous carbon with tailored pore size," *Microscopy and Microanalysis*, vol. 19, no. 3, pp. 745–750, 2013.

[31] S. Liu, Y. Yin, K. S. Hui, K. N. Hui, S. C. Lee, and S. C. Jun, "Nickel hydroxide/chemical vapor deposition-grown graphene/nickel hydroxide/nickel foam hybrid electrode for high performance supercapacitors," *Electrochimica Acta*, vol. 297, pp. 479–487, 2019.

[32] B. K. Singh, A. Shaikh, R. O. Dusane, and S. Parida, "Nanoporous gold-nitrogen-doped carbon nano-onions all-solid-state micro-supercapacitor," *Nano-Structures & Nano-Objects*, vol. 17, pp. 239–247, 2019.

[33] X. Shen, Y. Li, T. Qian et al., "Lithium anode stable in air for low-cost fabrication of a dendrite-free lithium battery," *Nature Communications*, vol. 10, no. 1, p. 900, 2019.

[34] X. Liu, M. N. Marlow, S. J. Cooper et al., "Flexible all-fiber electrospun supercapacitor," *Journal of Power Sources*, vol. 384, pp. 264–269, 2018.

[35] S. Zhou, D. Liu, Y. Cai, Y. Yao, and Z. Li, "3D characterization and quantitative evaluation of pore-fracture networks of two Chinese coals using FIB-SEM tomography," *International Journal of Coal Geology*, vol. 174, pp. 41–54, 2017.

[36] N. Ogihara, Y. Ozawa, and O. Hiruta, "A self-assembled intercalated metal-organic framework electrode with outstanding area capacity for high volumetric energy asymmetric capacitors," *Journal of Materials Chemistry A*, vol. 4, no. 9, pp. 3398–3405, 2016.

[37] S. Vierrath, L. Zielke, R. Moroni et al., "Morphology of nanoporous carbon-binder domains in Li-ion batteries—a FIB-SEM study," *Electrochemistry Communications*, vol. 60, pp. 176–179, 2015.

[38] M. Zhao, B. Ming, J.-W. Kim et al., "New insights into subsurface imaging of carbon nanotubes in polymer composites via scanning electron microscopy," *Nanotechnology*, vol. 26, no. 16, article 169601, 2015.

[39] S. K. Eswara-Moorthy, P. Balasubramanian, W. van Mierlo et al., "An in situ SEM-FIB-based method for contrast enhancement and tomographic reconstruction for structural quantification of porous carbon electrodes," *Microscopy and Microanalysis*, vol. 20, no. 5, pp. 1576–1580, 2014.

[40] A. Yürüm, Z. Ö. Kocabaş-Ataklı, M. Sezen, R. Semiat, and Y. Yürüm, "Fast deposition of porous iron oxide on activated carbon by microwave heating and arsenic (V) removal from water," *Chemical Engineering Journal*, vol. 242, pp. 321–332, 2014.

[41] R. C. Rodriguez, A. B. Moncada, D. F. Acevedo, G. A. Planes, M. C. Miras, and C. A. Barbero, "Electroanalysis using modified hierarchical nanoporous carbon materials," *Faraday Discussions*, vol. 164, pp. 147–173, 2013.

[42] S. Thiele, T. Fürstenhaupt, D. Banham et al., "Multiscale tomography of nanoporous carbon-supported noble metal catalyst layers," *Journal of Power Sources*, vol. 228, pp. 185–192, 2013.

[43] A. P. Cocco, G. J. Nelson, W. M. Harris et al., "Three-dimensional microstructural imaging methods for energy materials," *Physical Chemistry Chemical Physics*, vol. 15, no. 39, pp. 16377–16407, 2013.

[44] T. L. Burnett, R. Kelley, B. Winiarski et al., "Large volume serial section tomography by Xe plasma FIB dual beam microscopy," *Ultramicroscopy*, vol. 161, pp. 119–129, 2016.

[45] M. Cantoni and L. Holzer, "Advances in 3D focused ion beam tomography," *MRS Bulletin*, vol. 39, no. 4, pp. 354–360, 2014.

[46] Y. Song, C. A. Davy, D. Troadec, and X. Bourbon, "Pore network of cement hydrates in a high performance concrete by 3D FIB/SEM—implications for macroscopic fluid transport," *Cement and Concrete Research*, vol. 115, pp. 308–326, 2019.

[47] D. Wei, S. Jacobs, S. Modla et al., "High-resolution three-dimensional reconstruction of a whole yeast cell using focused-ion beam scanning electron microscopy," *BioTechniques*, vol. 53, no. 1, pp. 41–48, 2012.

[48] Y. Zhang, M. Dong, S. Zhu, C. Liu, and Z. Wen, "MnO_2@ colloid carbon spheres nanocomposites with tunable interior architecture for supercapacitors," *Materials Research Bulletin*, vol. 49, pp. 448–453, 2014.

[49] G. Brus, H. Iwai, M. Mozdzierz et al., "Combining structural, electrochemical, and numerical studies to investigate the relation between microstructure and the stack performance," *Journal of Applied Electrochemistry*, vol. 47, no. 9, pp. 979–989, 2017.

[50] R. S. Devarapalli, A. Islam, T. F. Faisal, M. Sassi, and M. Jouiad, "Micro-CT and FIB–SEM imaging and pore structure characterization of dolomite rock at multiple scales," *Arabian Journal of Geosciences*, vol. 10, no. 16, p. 361, 2017.

[51] M. Kishimoto, *Three-Dimensional Microstructure of Solid Oxide Fuel Cell Anode: Observation, Quantification, and Application to Numerical Analysis*, Kyoto University, Kyoto, Japan, 2013.

[52] P. Bala, K. Tsyrulin, H. Jaksch, and M. Stepien, "3D reconstruction and characterization of carbides in Ni-based high carbon alloy in a FIB-SEM system," *International Journal of Materials Research*, vol. 106, no. 7, pp. 764–770, 2015.

[53] D. A. Saab, P. Basset, F. Marty, D. E. Angelescu, and M. Trawick, "Accurate 3D reconstruction of silicon micro/nanostructures, based on high resolution FIB-SEM tomography: application to black silicon," in *Proceedings of the 2014 Symposium on Design, Test, Integration and Packaging of MEMS/MOEMS (DTIP)*, pp. 1–4, Cannes, France, April 2014.

[54] E. L. Solla, L. Micheron, P. Yot, J. Méndez, and P. Horcajada, "3D reconstruction and porosity study of a hierarchical porous monolithic metal organic framework by FIB-SEM nanotomography," *Microscopy and Microanalysis*, vol. 22, no. S4, pp. 4-5, 2016.

[55] S. Liu, L. Sun, J. Gao, and K. Li, "A fast curtain-removal method for 3D FIB-SEM images of heterogeneous minerals," *Journal of Microscopy*, vol. 272, no. 1, pp. 3–11, 2018.

[56] Y. Katayanagi, T. Shimizu, Y. Hashimasa, N. Matsushita, Y. Yamazaki, and T. Yamaguchi, "Cross-sectional observation of nanostructured catalyst layer of polymer electrolyte fuel cell using FIB/SEM," *Journal of Power Sources*, vol. 280, pp. 210–216, 2015.

[57] A. Etiemble, A. Tranchot, T. Douillard, H. Idrissi, E. Maire, and L. Roué, "Evolution of the 3D microstructure of a Si-based electrode for Li-ion batteries investigated by FIB/SEM tomography," *Journal of the Electrochemical Society*, vol. 163, no. 8, pp. A1550–A1559, 2016.

[58] Z. Liu, Y.-C. K. Chen-Wiegart, J. Wang, S. A. Barnett, and K. T. Faber, "Three-phase 3D reconstruction of a $LiCoO_2$ cathode via FIB-SEM tomography," *Microscopy and Microanalysis*, vol. 22, no. 1, pp. 140–148, 2016.

[59] G. Gaiselmann, M. Neumann, L. Holzer, T. Hocker, M. R. Prestat, and V. Schmidt, "Stochastic 3D modeling of $La_{0.6}Sr_{0.4}CoO_{3-\delta}$ cathodes based on structural segmentation of FIB-SEM images," *Computational Materials Science*, vol. 67, pp. 48–62, 2013.

[60] S. Ghosh, H. Ohashi, H. Tabata, Y. Hashimasa, and T. Yamaguchi, "Microstructural pore analysis of the catalyst layer in a polymer electrolyte membrane fuel cell: a combination of resin pore-filling and FIB/SEM," *International Journal of Hydrogen Energy*, vol. 40, no. 45, pp. 15663–15671, 2015.

[61] H. Aslannejad, S. M. Hassanizadeh, A. Raoof, D. A. M. de Winter, N. Tomozeiu, and M. T. van Genuchten, "Characterizing the hydraulic properties of paper coating layer using FIB-SEM tomography and 3D pore-scale modeling," *Chemical Engineering Science*, vol. 160, pp. 275–280, 2017.

[62] N. Nan and D. B. DeVallance, "Development of poly(vinyl alcohol)/wood-derived biochar composites for use in pressure sensor applications," *Journal of Materials Science*, vol. 52, no. 13, pp. 8247–8257, 2017.

[63] A. Sheidaei, M. Baniassadi, M. Banu et al., "3-D microstructure reconstruction of polymer nano-composite using FIB-SEM and statistical correlation function," *Composites Science and Technology*, vol. 80, pp. 47–54, 2013.

[64] K. Hagita, T. Higuchi, and H. Jinnai, "Super-resolution for asymmetric resolution of FIB-SEM 3D imaging using AI with deep learning," *Scientific Reports*, vol. 8, no. 1, p. 5877, 2018.